# END-TO-END TRAJECTORY FOR CONJUNCTION CLASS MARS MISSIONS USING HYBRID SOLAR-ELECTRIC/CHEMICAL TRANSPORTATION SYSTEM

**Patrick R. Chai**[*], **Raymond G. Merrill**[*], **and Min Qu**[†]

NASA's Human Spaceflight Architecture Team is developing a reusable hybrid transportation architecture in which both chemical and solar-electric propulsion systems are used to deliver crew and cargo to exploration destinations. By combining chemical and solar-electric propulsion into a single spacecraft and applying each where it is most effective, the hybrid architecture enables a series of Mars trajectories that are more fuel efficient than an all chemical propulsion architecture without significant increases to trip time. The architecture calls for the aggregation of exploration assets in cis-lunar space prior to departure for Mars and utilizes high energy lunar-distant high Earth orbits for the final staging prior to departure. This paper presents the detailed analysis of various cis-lunar operations for the EMC Hybrid architecture as well as the result of the higher fidelity end-to-end trajectory analysis to understand the implications of the design choices on the Mars exploration campaign.

## INTRODUCTION

The National Aeronautics and Space Administration (NASA) is currently developing options for potential future paths as part of an Evolvable Mars Campaign[1] (EMC) that expands human presence from Low Earth Orbit (LEO) into the solar system and to the surface of Mars. The strategic principles set forth for the EMC dictate that the journey to Mars involves an incremental buildup of capabilities while fielding interesting and exciting human space missions at a defined cadence without an increase to current funding levels. The resulting systems must be part of an evolvable multi-use infrastructure that provides significant opportunities for commercial and international involvement based on International Space Station (ISS) agreements and capabilities. These campaigns begin with Earth reliant missions to expand the knowledge of operations in space, continue with missions in cis-lunar space for testing and certification of required technologies, and ultimately result in Earth independent missions and long duration stays on the Martian surface.

Many different mission design concepts have been studied and proposed over the past three decades,[2–4] and many more are currently being investigated. In the majority of these studies, chemical propulsion has been assumed for the crewed Mars missions because solar electric propulsion, despite being much more fuel efficient, produces less thrust and is more suitable for cargo predeployment missions when the transit time can be much longer. NASA's Human spaceflight Architecture Team (HAT) is currently developing a new hybrid transportation architecture in which both chemical and electric propulsion are combined in an integrated design.[5] By combining chemical

[*]Aerospace Engineer, Space Mission Analysis Branch, NASA Langley Research Center, Hampton, VA 23681 USA
[†]Staff Scientist, Analytical Mechanics Associates, Inc., Hampton, VA 23666 USA
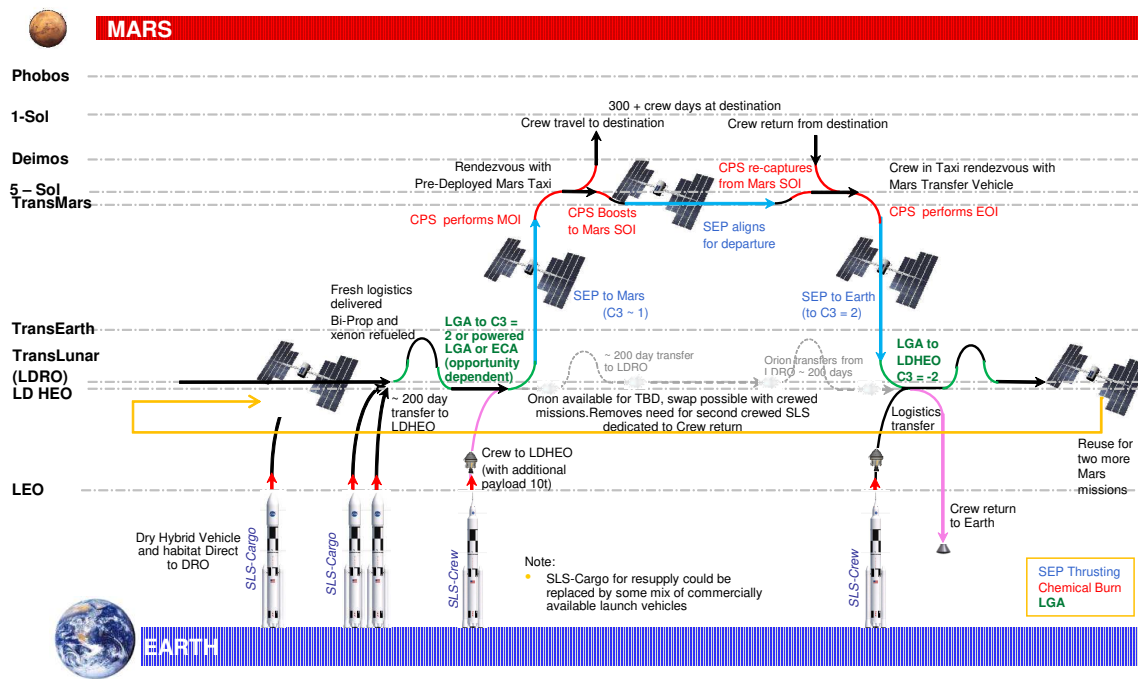
**Figure 1. Mars Hybrid Crew Mission Concept of Operation**

and solar-electric propulsion (SEP)[6,7] into a single spacecraft and applying each where it is most effective, the hybrid architecture enables a series of Mars trajectories that are more fuel efficient than an all chemical propulsion architecture without significant increases to trip time. The hybrid style trajectory allows the spacecraft to complete the round-trip journey to/from Mars in less than 1,100 days, which enables the reuse of the transportation system for multiple trips and eliminates the need to develop separate transportation systems for crew and cargo. For the hybrid transportation system, a series of trajectories were designed to minimize the propulsive energy required.

This paper presents the detailed analysis of various cis-lunar operations for the EMC Hybrid architecture. The results from these analysis provided estimates of performance requirements for system level trades and sizing. The EMC Hybrid interplanetary trajectory analysis was presented at the AIAA SPACE 2015 Conference,[8,9] while the Mars sphere of influence trajectory analysis was presented at the 2015 AAS Astrodynamics Specialist Conference.[10] The final end-to-end detailed trajectory is also presented in this paper for the EMC Hybrid 2039 mission opportunity.

## HYBRID TRANSPORTATION ARCHITECTURE

The initial Hybrid crew mission is depicted in Figure 1. Additional crew missions that reuse the integrated Mars spaceship begin with the vehicle in Lunar Distant Retrograde Orbit (LDRO) after the previous use. The crewed Mars mission begins with initial deployment and checkout of the integrated Hybrid Propulsion Stage (HPS) and the deep space transit habitat.[11] The stack is launched on a NASA Space Launch System (SLS) directly to a characteristic energy (C3) of -2 $km^3/s^2$, targets a Lunar Gravity Assist (LGA) and performs a six months weak stability boundary transit to a stable LDRO. A transfer orbit with C3 of -2 $km^3/s^2$ has apogee altitude roughly equal to the moon's orbit. Upon arrival in a LDRO, the HPS/Habitat stack rendezvous with existing cis-

lunar infrastructure, and resupply modules are launched (or are already waiting in LDRO) to transfer propellant and logistics required for the Mars missions. The transit of the resupply modules from Earth to LDRO requires a more direct transit as compared to the Hybrid's weak stability transit due to the limited lifetime of the vehicle. Depending on the launch opportunity and the performance capability of the resupply module, a direct transit or a powered LGA transit is utilized.

After the HPS/Habitat stack has been fully fueled and stocked with logistics, the stack performs another six month weak stability boundary transit from LDRO to lunar distant high Earth orbit (LDHEO) via a solar perturbation loop with a pair of LGAs. The Mars crew is launched on an SLS directly to the LDHEO, where they rendezvous with the HPS/habitat stack, transfer final logistics, and depart Earth in the HPS/habitat stack to Mars. From LDHEO, one or two LGA propels the crewed HPS stack to a C3 of +2 $km^3/s^2$. After Earth departure, the SEP system produces thrust in high thrust mode (2,000 seconds specific impulse) for much of the interplanetary trajectory to increase the vehicle's orbital energy to reach Mars. The crewed HPS stack arrives at Mars 300-400 days after Earth departure targeting a Mars close approach at 250 km altitude. The Hybrid's chemical engines performs a three-burn insertion maneuver to capture into a highly elliptical Mars orbit with a period of 5-Sol.

Upon arrival at Mars, a pre-deployed Mars taxi or a lander rendezvous with the crew HPS stack, then transfers the crew to their exploration destination. After the crew departs for their destination, the un-crewed HPS stack performs a series of maneuvers to reorient itself into the proper orbit for the return trip. After a minimum stay of 300 days in the Martian sphere of influence, the crew completes its exploration mission and returns to the HPS stack using the Mars taxi or a Mars ascent stage. From there, the HPS performs another three-burn maneuver to depart Mars. After Mars departure, the SEP thrusters uses high efficiency mode (3,000 seconds specific impulse) to reduce the spacecraft's energy to target an Earth arrival C3 of less than +2 $km^3/s^2$. The stack captures back into LDHEO via one or two LGA sequence similar to Earth departure, but in reverse.

An SLS launches an empty Orion to LDHEO to rendezvous with the crewed HPS stack and return the crew to Earth. After crew return, the HPS stack transits from LDHEO to LDRO using either a slow transfer ($\approx$ 6 months) or fast transfer ($\approx$ 10 days) depending on the departure window and fuel availability of the next mission. The fast transfer would require additional fuel to be carried by the SLS that brought the empty Orion capsule. Once in LDRO, the HPS rendezvous with existing cis-lunar infrastructure to perform refuel and resupply activities in preparation for the next trip to Mars.

## TRANSFERS BETWEEN EARTH AND MOON

NASA's Evolvable Mars Campaign calls for the aggregation of exploration assets in cis-lunar space prior to departure for Mars. The aggregation of exploration assets in cis-lunar space allows for rendezvous with pre-positioned assets during the Proving Ground[12] phase of the campaign, reduces the cost of the orbital maintenance, and improve the lifetime of the exploration assets by minimizing the time spend in the Van Allen radiation belt and the micrometeorites and orbital debris field. The Hybrid Transportation Architecture utilizes both LDRO and LDHEO for exploration assets aggregation. LDRO is utilized for long duration storage of assets and refueling and resupply operations. LDHEO is utilized for crew rendezvous and final phasing for departure and arrival via LGAs.
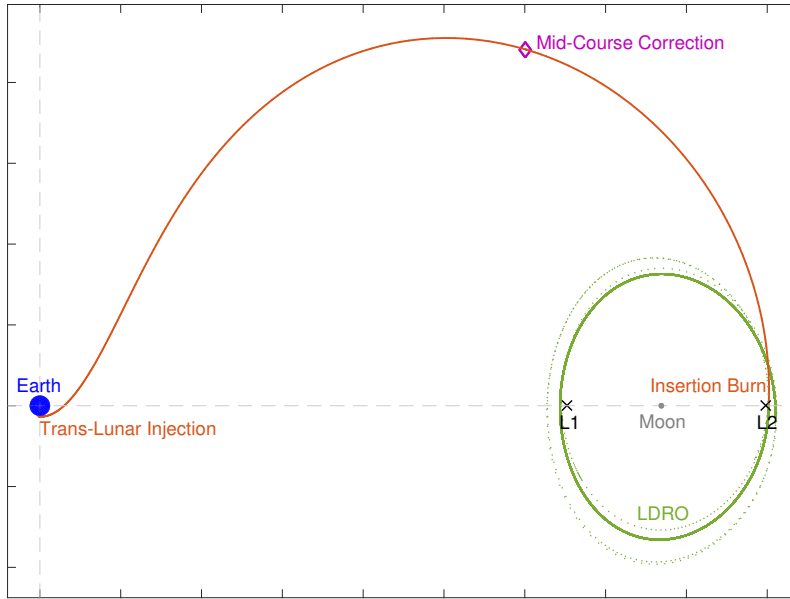
**Figure 2. Direct Far-Side Injection into Lunar Distant Retrograde Orbit Trajectory in Earth-Moon Two-Body Rotating and Pulsating Reference Frame**
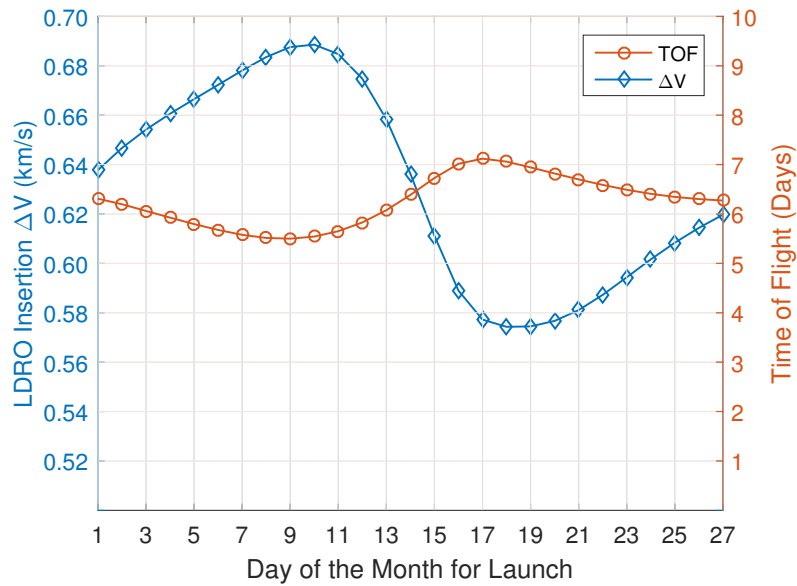


**Figure 3. $\Delta V$ and Time of Flight for Direct Far-Side Injection into Lunar Distant Retrograde Orbit as Function of Lunar Phasing**

**Direct Insertion to LDRO**

The transfer and insertion of exploration assets into LDRO can be achieved in different ways depending on mission requirements. Figure 2 shows a direct injection into LDRO in the Earth-Moon two-body rotating frame. The launch vehicle launches the payload to trans-Lunar injection condition with C3 of greater than -2 $km^3/s^2$. A C3 greater than -2 $km^3/s^2$ has apogee altitude beyond the Moon's orbit. In the example shown in the figure, the launch vehicle deliver the payload to target a far-side injection into LDRO near the Earth-Moon L2 point. The LDRO shown in Figure 2 and assumed as the baseline for the EMC Hybrid architecture has a half width of 70,000 km. This LDRO is chosen as the baseline because it is highly stable and analysis have shown that it requires little to no orbital maintenance for over 100 years. During the transit from Earth to insertion, the payload has the opportunity to perform a mid-course correct burn to adjust the trajectory and clean up any injection error that the launch vehicle imparted. Assuming the launch vehicle performs the injection burn, the payload is only responsible for the mid-course correction and the insertion maneuver. The cost of the direct far-side injection is a function of the time of the month in which the launch occurs.

Figure 3 shows the $\Delta V$ and time of flight of the direct far-side injection into LDRO as a function of the day of the month in which the launch of the spacecraft occurs. The LDRO is defined in the Earth-Moon rotating frame, which oscillates with the varying Earth-Moon distance. When the Moon is at apogee, the vehicle must travel farther to insert into the LDRO than when the Moon is at perigee. This variation has an impact on the total propulsive requirements for the insertion. As the figure show, the total transit time to LDRO varies between 5.5 to 7 days while the $\Delta V$ varies between 570 m/s to 690 m/s. The time of flight and $\Delta V$ are negatively correlated for the direct far-side injection. Ideally, the mission can target the launch to minimize the $\Delta V$; however, if the spacecraft is only designed to perform the minimum $\Delta V$ required, a launch scrub can cause a 28 day delay in the delivery of the asset into LDRO. This result is similar to those shown by Capdevila, Guzzetti, and Howell.[13]

**LDRO Insertion via PLGA**

An alternate option for LDRO insertion is shown in Figure 4. For this trajectory, either the launch vehicle launches the payload to trans-lunar injection or the spacecraft is already in a LDHEO. Both of these scenario requires the spacecraft to have a orbital C3 of -2 $km^3/s^2$ to reduce the $\Delta V$ cost of targetting a LGA. For the Earth launched scenario, instead of targeting a LDRO insertion near the Earth-Moon L2 point, it targets a lunar close approach. This reduces the performance requirement on the launch vehicle, as it would only require the launch vehicle to deliver the payload to a C3 of -2 $km^3/s^2$. For the scenario in which the spacecraft is already in a LHDEO, a small phasing maneuver is required to target the LGA. Regardless of the initial scenario, the spacecraft performs a propulsive maneuver at the lunar close approach to target a LDRO insertion at at a later time. The timing and location of the insertion burn is epoch dependent. In the example shown in the figure, the insertion occurs roughly half orbit later before the orbit reaches the Earth-Moon L2 point.

The most immediate benefit of this trajectory is by reducing the launch vehicle performance requirement: additional payload mass can be delivered to the LGA condition as compared to the direct insertion near L2. This also reduces the propulsive requirement for the scenario in which the spacecraft is already in LDHEO, as it requires only phasing of the orbit to catch the LGA rather than a large propulsive burn to increase the orbit's apogee to target the direct insertion. Additionally, as shown in Figure 5, the powered LGA and insertion $\Delta V$ is less than the direct insertion $\Delta V$. The
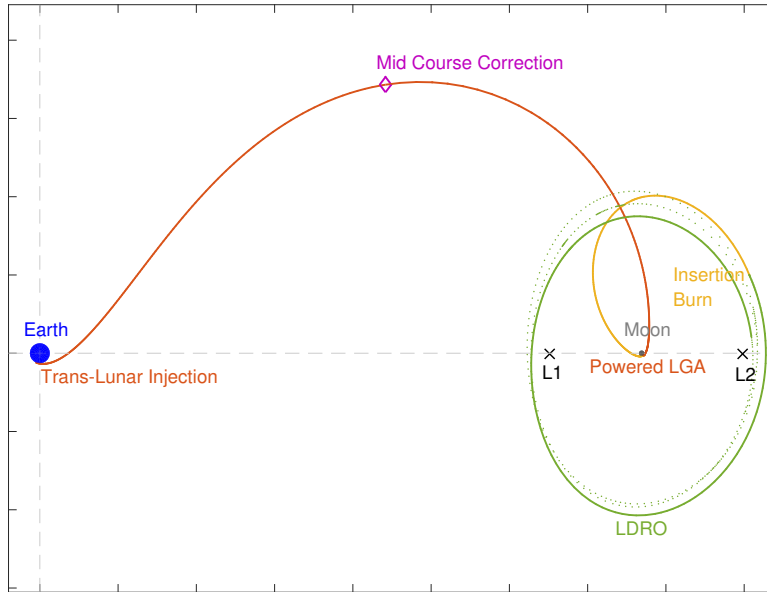
**Figure 4.   Lunar Distant Retrograde Orbit Injection via a Powered Lunar Gravity Flyby in Earth-Moon Two-Body Rotating and Pulsating Reference Frame**
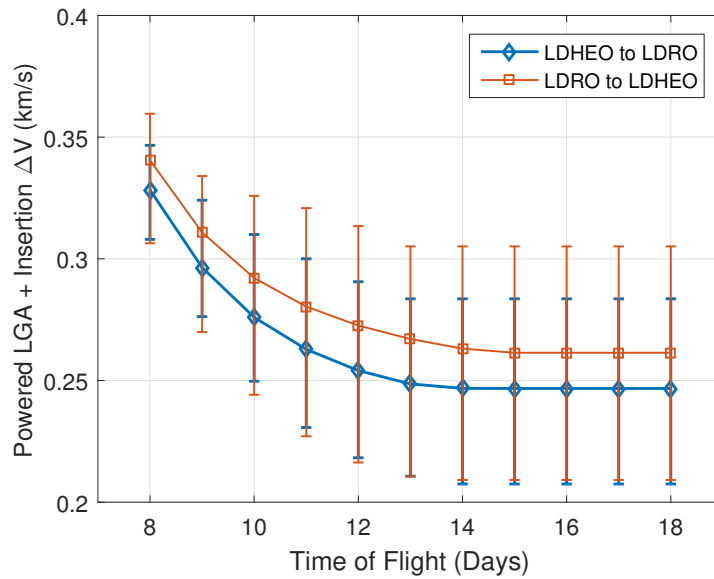


**Figure 5.  Minimum, Mean, and Maximum $\Delta V$ for Transfer between Lunar Distant High Earth Orbit and Lunar Distant Retrograde Orbit with a Powered Lunar Gravity Assist Maneuver as Function of Total Time of Flight**

Figure shows the minimum, maximum, and average $\Delta V$ for transfers between LDRO and LDHEO as function of time of flight. The time of flight become more of an independent variable in this trajectory because of the added Powered Lunar Gravity Assist (PLGA) burn, which give an extra degree of freedom to target the LDRO insertion. Longer duration direct insertion is possible but not necessarily more cost effective. The variation of the $\Delta V$ for each time of flight is due to the time of month in which the maneuver occurs. As the figure shows, shorter time of flight requires higher $\Delta V$ for the PLGA and insertion. The time of flight for the PLGA insertion is higher than the direct insertion, ranging from 8 to 18 days. As the time of flight increase, the total $\Delta V$ for the PLGA insertion decreases; however, the curves flattens out when TOF becomes greater than 14 days. At 14 days, the total $\Delta V$ required for the maneuver ranges from 210 m/s to 310 m/s, which represents a saving of over 50% as compared to the direct insertion maneuver. Even the 8 day PLGA transfer can provide $\Delta V$ saving of 250-300 m/s as compared to the direct injection maneuver.

**LDRO Insertion via Weak Stability Boundary**

A third option for LDRO to LDHEO transfer is a weak stability boundary (WSB) transfer which utilizes solar perturbations to increase or decrease orbital energy coupled with LGAs to bring insert or depart LDRO. The WSB transfer is described in detail by Belbruno[14] and Parker[15,16] as the low energy Ballistic Lunar Transfer (BLTs). For the EMC Hybrid architecture, to minimize the propulsive requirements, the low energy transfer maneuvers involves two LGAs. The first LGA propels the spacecraft away from the Earth-Moon system to near the edge of the Earth-Moon sphere of influence so that it can utilizes solar perturbation and a small burn with either chemical or solar electric propulsion to reorient the trajectory for a second LGA that will capture into LDRO. The same maneuver can be performed in reverse to transit from LDRO to LDHEO. The total time of flight for the maneuver is nearly 180 days due to the time it takes to travel to the edge of the Earth-Moon sphere of influence, but this trajectory only requires a $\Delta V$ of less than 80 m/s.[10] Time permitting, this is the preferred method for transfers between LDRO and LDHEO for the EMC Hybrid architecture as it minimizes the propulsive requirement.

**LDRO MAINTENANCE AND PHASING FOR RENDEZVOUS**

The selection of the LDRO for aggregation of exploration assets is motivated by its stability and high energy state which allow for lower energy departure from the Earth-Moon system as compared to departures from low Earth orbit. The stability of the LDRO is dependent on the amplitude of the LDROs.[13] LDRO with very small amplitudes can be regarded as low lunar orbit, as the third body effect from the Earth is dominated by the gravitational pull of the moon. As the amplitude increases, the balance between the gravitational pull of the Moon and the Earth can make the orbit very stable. Figure 6 shows the 70,000 km LDRO propagated for 50 years staring with a 2020 epoch. This LDRO does exhibit small variation to its amplitude during the simulation, however, it remains stable in the Earth-Moon system through the full simulation provided there are no external artificial forces acting on the system. The stability of this orbit makes it ideal for long term aggregation point for exploration assets that can take several years to assemble prior to its deployment.

The benefit provided by the LDRO is not without cost. As discussed in the previous section, there is a performance cost associated with inserting and departing from the LDRO aggregation orbit. Additionally, any exploration asset that travels to LDRO would require phasing and rendezvous with pre-deployed assets. The LDRO is stable provided there are no external forces acting on the spacecraft; however, small perturbations to the orbital velocity can result in large deviations from
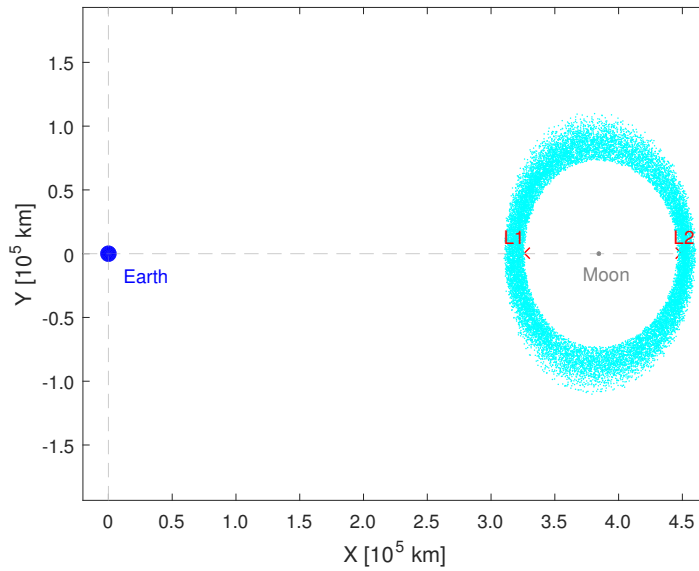
**Figure 6.  25 Year Propagation of 70,000 km Amplitude Lunar Distant Retrograde Orbit with No Orbital Maintenance in Earth-Moon Two-Body Rotating and Pulsating Reference Frame**
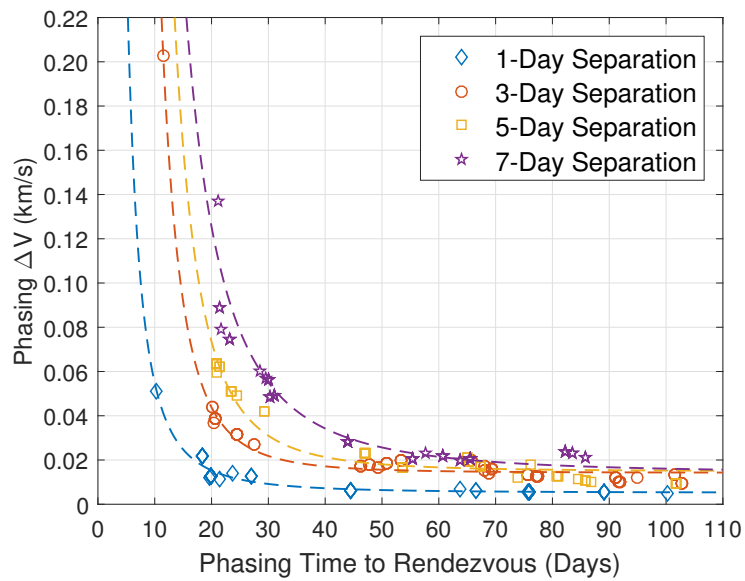


**Figure 7.  LDRO Phasing $\Delta V$ as Function of Insertion Separation Distance and Time to Rendezvous**

the stable orbit. Thus, the phasing and rendezvous of elements in LDRO must be more precise as compared to rendezvous in low Earth orbit. The cost of the phasing and rendezvous of elements in LDRO is a function of both the separation distance and the total time available for phasing. There are an infinite number of distant retrograde orbits that can be utilized for phasing, and as shown in Figure 6, these orbit have slight variation in their amplitude. Thus, given enough time, one can find and utilize an optimal orbit for phasing to the desired orbit.

Figure 7 shows the total phasing $\Delta V$ as function of both the separation distance and the time required to rendezvous with a target in the 70,000 km LDRO. The separation distance is defined in terms of time. The orbital period of the 70,000 km LDRO is roughly 14 days, thus a 7-day separation constitute the worse case scenario. As the figure shows, the phasing time required to rendezvous has a large impact on the total phasing $\Delta V$. If more than 40 days are available for phasing, the total $\Delta V$ for phasing, regardless of the initial separation distance, can be less than 30 m/s. However, if faster phasing is required, then the phasing $\Delta V$ can be as high as 200+ m/s for the worse case separation. The initial separation distance is a function of the departure timing of the transit from Earth (or LDHEO) into the LDRO. As discussed in the previous section, the timing of the transit has an impact on the insertion $\Delta V$ due to the oblateness of the Moon's orbit. Thus, the timing of the insertion and the phasing separation distance form a coupled optimization problem. Ideally, one can time the departure for the transit to LDRO to minimize the transit $\Delta V$ and insert into LDRO with minimal separation from the target vehicle, but in reality, this may not be possible for all opportunities. From a mission planning perspective, it would be ideal to budget for more phasing time to rendezvous than more $\Delta V$, as the former reduces the the performance requirements for the propulsion system. For disposable refueling missions, the trade-off between $\Delta V$ and total mission lifetime will be critical to optimize the overall refuel and resupply strategy.

**LDHEO MAINTENANCE AND PHASING FOR DEPARTURE**

LDHEO is utilized in the EMC Hybrid Architecture as the final staging point for the crew and cargo spacecraft prior to departure for Mars, as well as the initial staging orbit for crew return. The baseline LDHEO has a perigee altitude of 407 km and an apogee altitude of 400,000 km. The high apogee altitude makes the orbit relatively unstable compared to normal Earth orbits as the gravitational pull from the Sun has more effect on the orbit's perigee altitude. The impact of the solar perturbation is highly coupled with the orientation of the LDHEO and the orbit's period. If the orbit's line of apsides is in an unfavorable orientation, the impact of the solar perturbation on the orbit's eccentricity can be much more dramatic than if the apsides is in a favorable orientation.

This effect can be observed in Figure 8, where the perigee altitude is plotted as a function of time and argument of periapsis for an LDHEO with peripasis altitude of 407 km, apoapsis altitude of 400,000 km, inclination of 28.5 degrees, and longitude of ascending node of 0 degrees at time zero (in J2000 Earth centered frame). The figure shows the variation of the perigee altitude behavior when the orbit is oriented differently with respect to the Sun. When the Sun is aligned with the perigee direction, the solar perturbation increase the perigee altitude and reduces the apogee altitude. Conversely, when the Sun is aligned with the apogee direction, the perigee altitude decreases and the apogee altitude increases. When the Sun is not aligned with the line of apsides, the effect of the solar perturbation on the orbital altitude is reduced but not diminished.

With a 407 km perigee LDHEO, the effect of the solar perturbation can cause significant instability to the orbit, as small reductions in the perigee altitude will result in atmospheric interface and trigger reentry. LDHEOs with higher perigee altitude do not significantly impact the effects of the
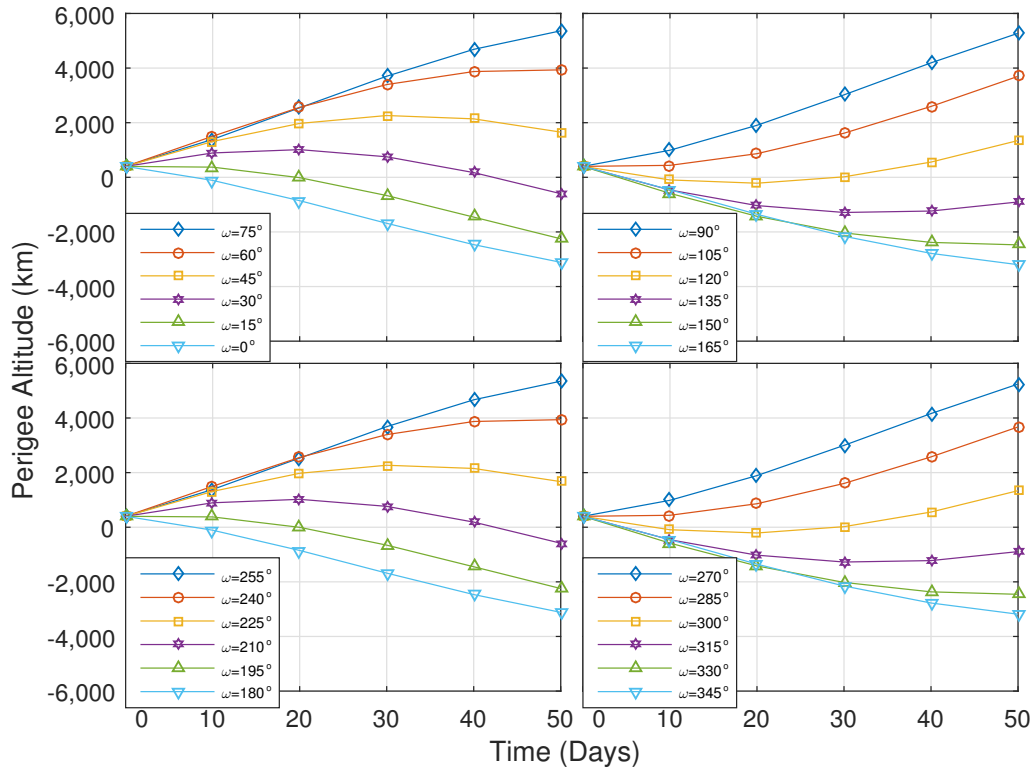
**Figure 8.** Periapsis Altitude as Function of Time for 407km x 400,000 km Lunar Distant High Earth Orbit with 28.5$^o$ Inclination and 0$^o$ Longitude of Ascending Node (in J2000 Earth Centered Frame) with Varying Argument of Periapsis ($\omega$)
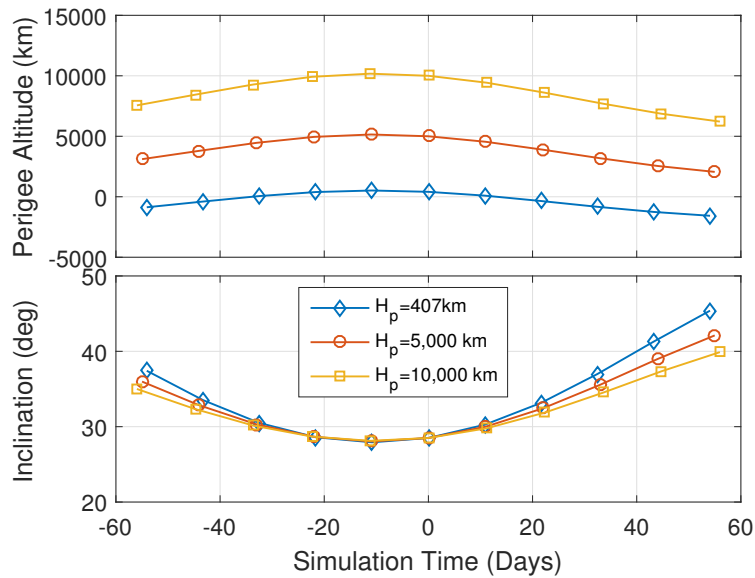


**Figure 9.** Lunar Distant High Earth Orbit (400,000 km Apogee Altitude) Inclination and Periapsis Altitude Propagation Over Time with 180 Degree Argument of Periapsis and 0 Degree Longitude of Ascending Node (in J2000 Earth Centered Frame)
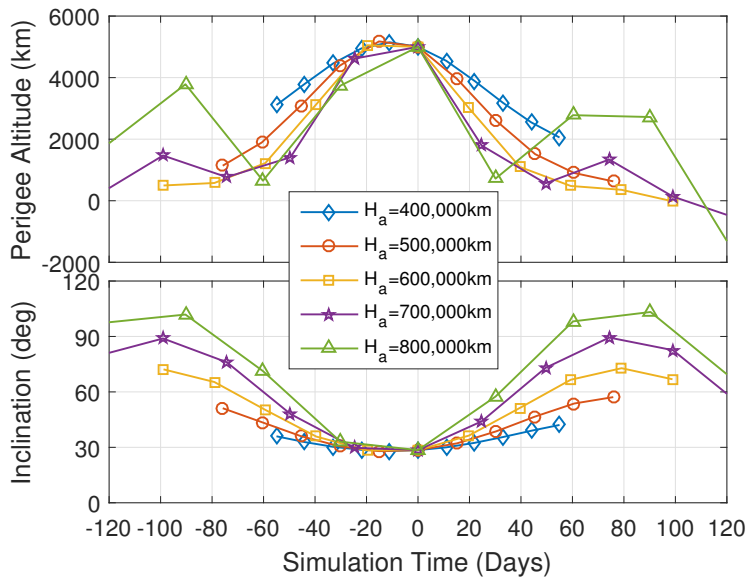
**Figure 10. Lunar Distant High Earth Orbit (5,000 km Perigee Altitude) Inclination and Periapsis Altitude Propagation Over Time with 180 Degree Argument of Periapsis and 0 Degree Longitude of Ascending Node**

solar perturbation. Figure 9 shows the propagation of three LDHEOs, all with 400,000 km apogee altitude, 0 degrees longitude of ascending node, and 180 degrees argument of periapsis in J2000 Earth centered frame. As the top figure shows, as the perigee altitude increases, the rate of the perigee altitude degradation does not change much. Starting at a higher perigee altitude allows for more time before the solar perturbation causes atmospheric interface. The bottom figure shows the effect of the solar perturbation on the inclination of the orbit. With the Sun not directly aligned with the line of apside, the solar perturbations affect the inclination of the orbit, increasing it by as much as 10 degrees in only 4 or 5 orbits. Increasing the perigee altitude of the LDEHO does not make a significant impact on the rate of the inclination change. To decrease the likelihood of atmospheric interface, it would appear that LDHEOs with higher perigee altitude are preferred, however, higher perigee altitudes put additional performance requirements on rendezvous with the crew vehicle.

For the EMC hybrid Mars architecture, the LDHEO serves as the final staging orbit prior to departure for Mars. The departure sequence requires the spacecraft in LDHEO to catch one or more LGAs for departure. Depending on the required departure velocity vector, the apogee altitude of the staging LDHEO can vary between one to two lunar distances. To understand the impact of higher apogee altitudes, Figure 10 shows the perigee altitude and inclination as function of time for LDHEO with 5,000 km perigee altitude, 0 degrees longitude of ascending node, and 180 degrees argument of periapsis. The simulation utilized a 5,000 km perigee altitude to better demonstrate the instability of the orbits, due to the inability for the simulation to propagate orbits with perigee altitude less than -3,678 km. Each data marker on the plots represents a single orbital period. As the perigee altitude increases, the stability of the LDHEO deteriorates accordingly. As the orbit moves farther away from Earth's gravity, the perturbation from the Sun increases to create higher instability in the orbit's altitude and inclination. For opportunities in which a higher apogee altitude is required, appropriate maintenance maneuvers must be planned to reduce the risk of atmospheric interface.
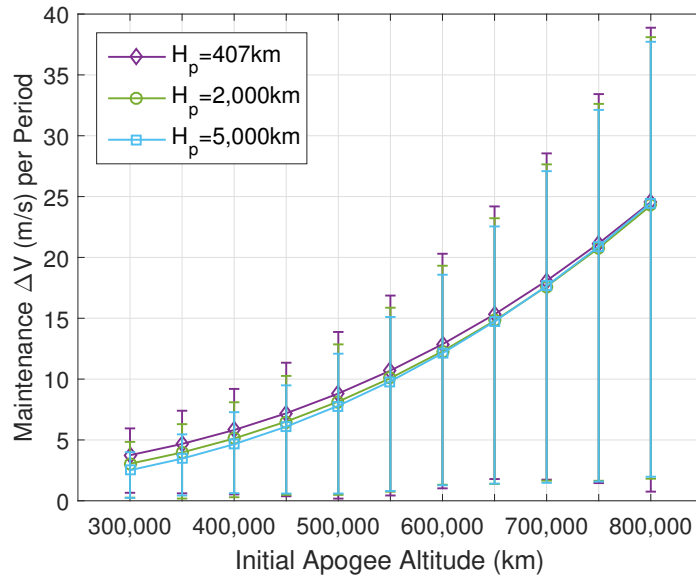
11

**Figure 11.  Lunar Distant High Earth Orbit Orbital Maintenance Cost**

To counter the instability of the LDHEO orbit, maintenance maneuvers are required.  The duration in which the spacecraft must be maintained in the LDHEO is dependent on the specific opportunity and the launch capability of the crew vehicle.  Launch of the crew to rendezvous with the pre-deployed spacecraft can suffer from delays due to various reasons, and thus the spacecraft must protect for multiple LDHEO periods to account for unforeseen delays.  To provide a baseline estimate of the total maintenance required for the LDHEO, a two burn maneuver is utilized to maintain the orbit's initial conditions.  The orbit is propagated for 1/2 period, where a perigee altitude and inclination maintenance maneuver is performed at apogee, then the orbit propagates another 1/2 period and a apogee altitude maintenance maneuver is performed.  Figure 11 shows the minimum, maximum, and average total $\Delta V$ required per orbit to maintain the LDHEO with the specified perigee altitude and 28.5 degrees inclination as a function of the initial apogee altitude. The variation of the maintenance $\Delta V$ is due to the different orientations of the LDHEO.

For the baseline 407 x 400,000 km altitude LDHEO, the maintenance cost ranges between 1 to 9 m/s per orbital period.  If one can choose the orientation of the LDHEO freely, the maintenance cost of the LDHEO can be optimized.  However, the orientation of the LDHEO is dictated by the required Earth departure (or arrival) velocity direction, so unless a detailed trajectory is available for the particular mission opportunity, the worse case $\Delta V$ must be utilized.  As the apogee altitude increases, the maintenance costs increase exponentially, with the worse case $\Delta V$ of around 40 m/s per period for a LDHEO that has an apogee altitude of twice lunar distance ( 800,000km).  Additionally, the dispersion of the maintenance cost increases as the apogee altitude increases, creating more uncertainty for the mission planning. If the campaign requires staging in LDHEO for multiple orbital periods, the $\Delta V$ cost can become cumbersome to the overall mission design. From a mission planning point of view, the average orbital maintenance $\Delta V$ per day can be used as preliminary estimate.  Even though the higher apogee altitude LDHEO has higher maintenance $\Delta V$ per orbit, the longer orbital period normalizes the value for comparison.  Overall, the average orbital maintenance cost is around 0.6 m/s per day, with a maximum cost of 1.3 m/s per day. Currently, the EMC mission
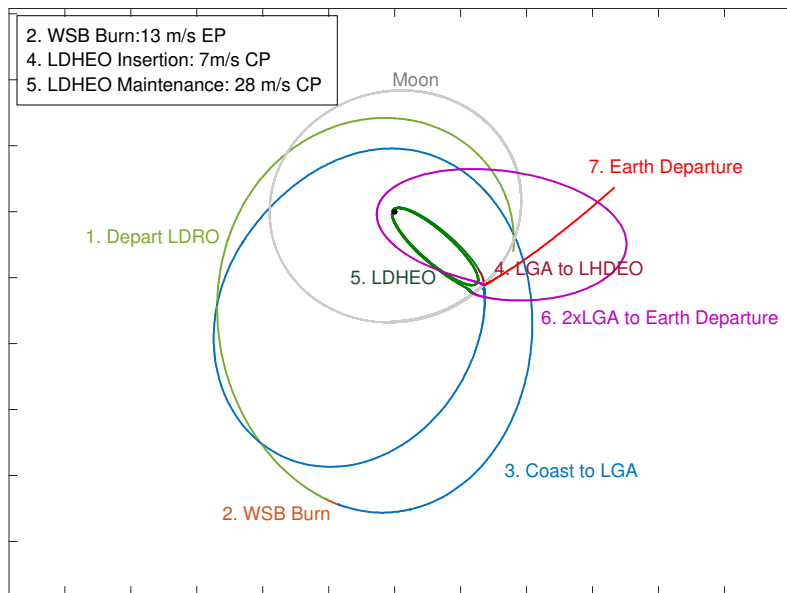
12

**Figure 12. 2039 EMC Hybrid Mars Mission Earth Departure Trajectory Sequence (Earth J2000)**

planning team is utilizing an orbital maintenance cost of 1 m/s per day as a preliminary estimate prior to detailed trajectory analysis.

**END-TO-END 2039 TRAJECTORY**

Combining the analysis compiled from this paper and the author's previous papers,[8–10] an end-to-end trajectory for the 2039 EMC Hybrid round-trip crew mission to Mars was compiled. The 2039 mission opportunity is the second crewed mission in the current EMC Hybrid architecture, with the first mission being the 2033 crewed mission to Phobos. For this trajectory, only the crew elements are considered, and the trajectory begins after the Hybrid spacecraft is fully refueled and resupplied for the mission opportunity.

Figure 12 shows the Earth departure sequence for the 2039 mission opportunity in Earth centered J2000 reference frame. After the Hybrid spacecraft completes its refueling and resupply operation, it departs the LDRO via the weak stability boundary trajectory after LGA. A mid-course correction maneuver of 13 m/s using the SEP system targets a second LGA, where small 7 m/s chemical burn inserts the spacecraft into the LDHEO. The LDHEO for this opportunity has a perigee altitude of 407 km and an apogee altitude of 365,000 km. The orientation of the LDHEO is such that the spacecraft will encounter the moon for a LGA maneuver after 2 orbital periods. The LDHEO has 28.5 degree inclination, 88.6 degree longitude of ascending node, and 53.9 degree argument of periapsis. During these 2 orbital periods, the total maintenance $\Delta V$ is 28 m/s, which translates to roughly 1.4 m/s per day. After two orbital periods in LDHEO, during which the crew is launched on an Orion vehicle and rendezvous with the Hybrid spacecraft, the Hybrid spacecraft catches two more LGAs to achieve its Earth departure condition with a departure C3 of 2 $km^3/s^2$.

Figure 13 shows the interplanetary trajectory from Earth to Mars for the EMC Hybrid 2039 crew mission in Sun centered J2000 frame. The Earth departure maneuver from Figure 12 targets a departure date of 08/04/2039. Once a departure C3 of 2 $km^3/s^2$ is achieved, the SEP thrusters
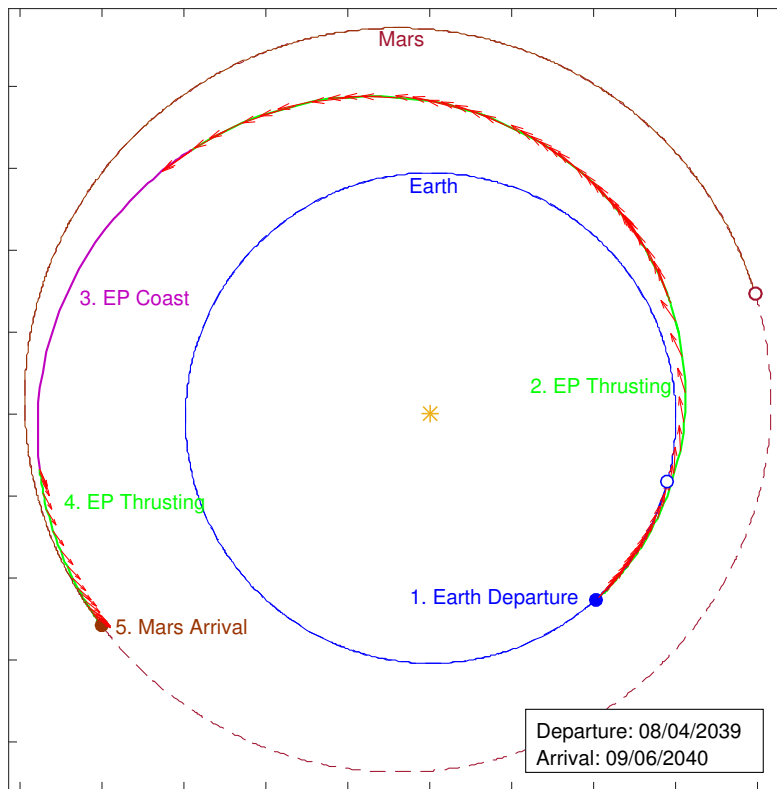
**Figure 13. 2039 EMC Hybrid Mars Mission Earth to Mars Outbound Interplanetary Trajectory (Sun J2000)**



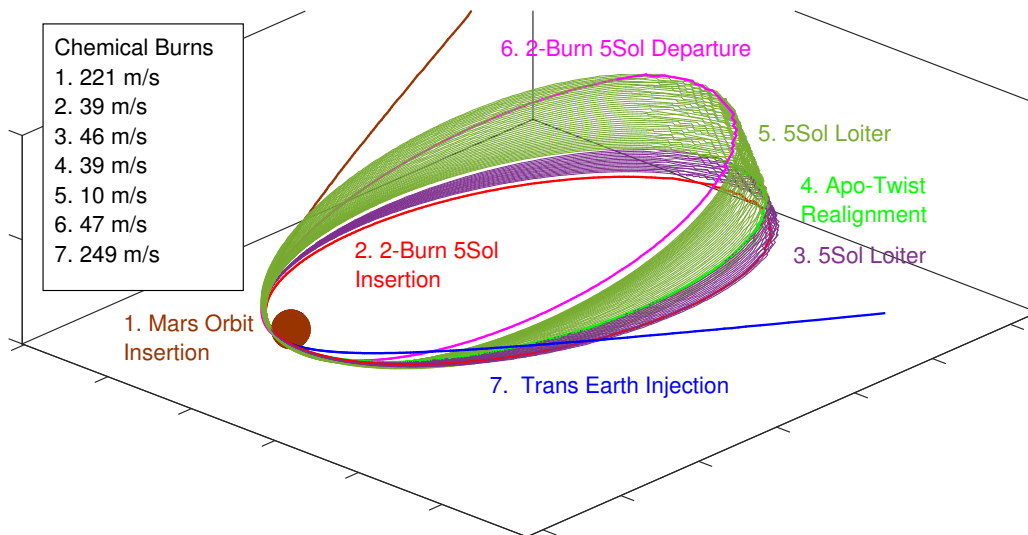**Figure 14. 2039 EMC Hybrid Mars Mission Mars Sphere of Influence Operation Trajectory Sequence (Mars J2000)**
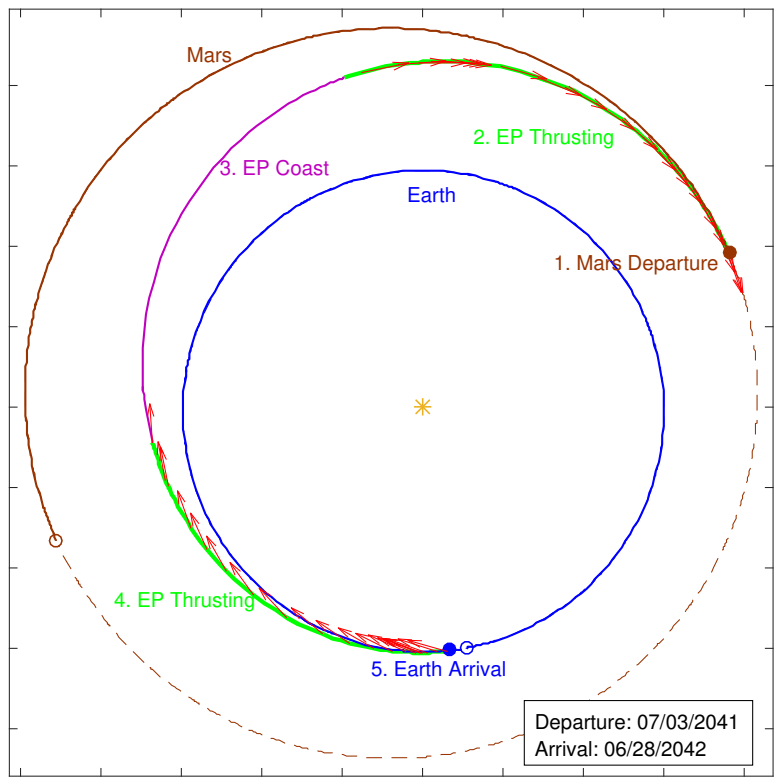
14

**Figure 15. 2039 EMC Hybrid Mars Mission Mars to Earth Inbound Interplanetary Trajectory (Sun J2000)**
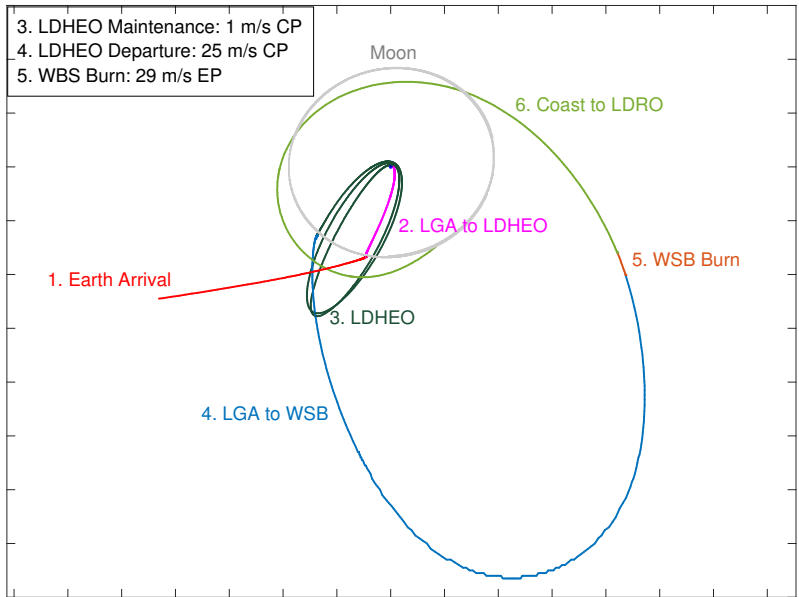


**Figure 16. 2039 EMC Hybrid Mars Mission Earth Arrival Trajectory Sequence (Earth J2000)**

begins thrusting continuously in high thrust mode (with 2,000 second specific impulse) for 225 days for a total effective $\Delta V$ of 2.7 km/s. Then the spacecraft coasts for 118 days before the SEP thrusters thrust for an additional 53 days and 386 m/s to target a Mars encounter on 09/06/2040. Total outbound interplanetary duration is 396 days with a total effective SEP $\Delta V$ of approximately 3.1 km/s.

Figure 14 shows the Mars sphere of influence trajectory for the Hybrid spacecraft in Mars centered J2000 frame. The spacecraft enters Mar's sphere of influence with incoming V-infinity of 1.20 km/s, right ascension of 110 degrees, and declination of -3.97 degrees. At Mars close approach, with a perigee altitude of 250 km, a 221 m/s chemical Mars orbit insertion burn is performed. After the initial orbit insertion burn, two additional orbit adjustments burns totaling 39 m/s are performed to insert into the 5-sol parking orbit. The spacecraft rendezvous with a pre-deployed lander, and the crew depart the spacecraft for their surface mission. The Hybrid spacecraft remains in the initial 5-sol orbit for 80 days, with an orbital maintenance cost of 46 m/s, before performing a 39 m/s re-orientation maneuver which realigns the orbital apside to prepare for eventual Mars departure. The maneuver is described by the apotwist[10] maneuver in the previous paper. The spacecraft loiters in the new 5-sol parking orbit for an additional 205 days, waiting for the crew to complete their surface mission, with an orbital maintenance cost of 10 m/s. After the crew returns from the surface, the spacecraft performs a three burn Mars departure maneuver. The first two maneuvers, totaling 47m/s, realign the orbit for the final trans-Earth injection maneuver. The trans-Earth injection maneuver is a 249 m/s burn, which results in a Mars departure V-infinity of 1.31 km/s with -118 degree right ascension and -2.31 degree declination. Total Mars sphere of influence stay time is 300 days, and total maneuver $\Delta V$ is 574 m/s all chemical.

Figure 15 show the interplanetary trajectory from Mars back to Earth in Sun centered J2000 frame. The trans-Earth injection occurs on 07/03/2041. After Mars departure, the SEP thrusts for 142 days continuously in high specific impulse mode (3,000 seconds), resulting in a total effective $\Delta V$ of 1.41 km/s. Then the spacecraft coasts for 125 days before the SEP thrusts for additional 93 for 1.48 km/s to target an Earth arrival on 06/28/2042. Total inbound interplanetary duration is 360 days with total effective SEP $\Delta V$ of approximately 2.90 km/s.

Finally, Figure 16 shows the Earth arrival sequence for the 2039 crew mission opportunity back in Earth centered J2000 frame. The incoming interplanetary velocity directly targets a LGA which provides a free insertion into a 407 x 666,000 km LDHEO. This particular LDHEO during this particular opportunity is relatively stable, only costing a total maintenence $\Delta V$ of less than 1 m/s for two orbital periods (48 days total). After the crew departs on a newly launched and rendezvoused Orion capsule, the Hybrid spacecraft departs the LDHEO with a small chemical burn of 25 m/s to target another weak stability boundary trajectory to LDRO. A mid-course correction burn of 29 m/s using the SEP thruster is required to target the final LGA for insertion into the LDRO, where the Hybrid spacecraft waits for refuel and resupply for the 2041 crew mission.

**SUMMARY**

Detailed analysis of the EMC Hybrid Transportation Architecture is underway by NASA's Human Exploration Architecture Team. Trajectory analysis of the cis-lunar operations presented in this paper defined additional requirements for the transportation architecture. Multiple options exist for the transit between Earth and cis-lunar staging orbits, and the $\Delta V$ costs associated with the transit are typically negatively correlated with time. A chemical propulsion system is required to make the propulsive maneuvers for short duration transits, while long duration transit can be feasible with a

low thrust solar electric propulsion system. The choice of the transit is dependent on the vehicle's design lifetime and the time available prior to the next mission. The orientation of the Earth-Moon system also has an impact on the transit time and cost. In addition, the phasing of assets in distant retrograde orbits is also dependent on the time available for phasing and the orbit insertion condition. The cis-lunar refueling and resupply infrastructure and operation is a closely coupled and complex problem that warrants further study.

Utilizing the cis-lunar space as staging grounds for the eventual Mars mission is critical in maintaining the transportation asset's lifetime for reusability and maintaining the asset's orbital energy. The use of the lunar distant high Earth orbit for final departure staging takes advantage of the asset's high energy state by decoupling the Earth reentry system from the transportation system. However, the asset's high energy state also equates to high orbital instability, resulting in an increased orbital maintenance cost. The time waiting for the crew launch and rendezvous can quickly become costly as the vehicle is fully loaded with fuel and logistics. The orientation of the orbit can have significant impact on the maintenance cost of the staging orbit; however, the orbit's orientation is dictated by the interplanetary departure and arrival conditions and cannot be chosen freely. The detailed end-to-end trajectory for the 2039 crew mission opportunity shows the drastic difference in the orbital maintenance cost for the high energy orbit. Refinement of the Hybrid spacecraft vehicle itself, as well as additional trajectory options and system level trades, are ongoing to further understand the impact of a fully reusable space transportation system on the Evolvable Mars Campaign.

## REFERENCES

[1] D. A. Craig, N. B. Herrmann, and P. A. Troutman, "The Evolvable Mars Campaign - Study Status," *IEEE Aerospace Conference*, March 2015. 2015-8.0101.

[2] Mars Architecture Steering Group and B. G. Drake, "Human Exploration of Mars Design Reference Architecture 5.0," Special Publication 2009-566, National Aeronautics and Space Administration, July 2009.

[3] D. O. Stanley, S. Cook, J. Connolly, J. Hamaker, M. Ivins, W. Peterson, J. Geffre, B. Cirillo, C. McClesky, J. Hanley, *et al.*, "NASA's Exploration System Architecture Study," Technical Memorandum 2005-214062, National Aeronautics and Space Administration, November 2005.

[4] J. Olson, "Human Exploration Framework Team Phase I Closeout," National Aeronautics and Space Administration, September 2, 2010.

[5] R. G. Merrill, N. Strange, M. Qu, and N. Hatten, "Mars Conjunction Crewed Missions with a Reusable Hybrid Architecture," *IEEE Aerospace Conference*, March 2015. 2015-8.0104.

[6] R. Hofer and A. Gallimore, "High-Specific Impulse Hall Thrusters, Part 1: Influence of Current Density and Magnetic Field," *Journal of Propulsion and Power*, Vol. 22, No. 4, 2006, pp. 721–731.

[7] R. Hofer and A. Gallimore, "High-Specific Impulse Hall Thrusters, Part 2: Efficiency Analysis," *Journal of Propulsion and Power*, Vol. 22, No. 4, 2006, pp. 732–740.

[8] P. R. Chai, R. G. Merrill, and M. Qu, "Mars Hybrid Propulsion System Trajectory Analysis Part I: Crew Missions," *AIAA SPACE 2015 Conference and Exposition, Pasadena, CA*, August 2015. AIAA 2015-4443.

[9] P. R. Chai, R. G. Merrill, and M. Qu, "Mars Hybrid Propulsion System Trajectory Analysis Part II: Cargo Missions," *AIAA SPACE 2015 Conference and Exposition, Pasadena, CA*, August 2015. AIAA 2015-4444.

[10] M. Qu, R. G. Merrill, P. R. Chai, and D. R. Komar, "Trajectory Designs for a Mars Hybrid Transportation Architecture," *2015 AAS/AIAA Astrydynamics Specialist Conference*, August 2015. AAS 15-552.

[11] M. A. Simon, S. I. Wald, A. Howe, and L. Toups, "Evolvable Mars Campaign Long Duration Habitation Strategies: Architectural Approaches to Enable Human Exploration Missions," *AIAA SPACE 2015 Conference and Exposition, Pasadena, CA*, 2015. AIAA 2015-4514.

[12] R. G. Merrill, P. R. Chai, and Min, "An Integrated Hybrid Transportation Architecture for Human Mars Expeditions," *AIAA SPACE 2015 Conference and Exposition, Pasadena, CA*, 2015. AIAA 2015-4442.

[13] L. Capdevila, D. Guzzetti, and K. C. Howell, "Various Transfer Options From Earth into Distant Retrograde Orbits in the Vicinity of the Moon," *AAS/AIAA Spaceflight Mechanics Meeting*, 2014. AAS 14-467.

[14] E. A. Belbruno and J. P. Carrico, "Calculation of Weak Stability Broundary Ballistic Lunar Transfer Trajectory," *ASIAA/AAS Astrodynamics Specialist Conference*, 2000. AIAA 2000-4142.

[15] J. S. Parker and G. H. Born, "Modeling a Low-Energy Ballistic Lunar Transfer Using Dynamical System Theory," *Journal of Spacecraft and Rockets*, Vol. 45, November-December 2008, pp. 1269–1281.

[16] J. S. Parker, *Low-Energy Ballistic Lunar Transfers*. PhD thesis, University of Colorado, 2007.